J Ther Eng, Vol. 10, No. 2, pp. 360−374, March, 2024

Journal of Thermal Engineering
Web page info: https://jten.yildiz.edu.tr
DOI: 10.18186/thermal.1448632

Journal of Thermal Engineering

Research Article

Enhancement in thermal and electrical characteristics of solar photovoltaic module through a direct contact water jacketed cooling system

Deepak Kumar SHARMA[1], Manish K RATHOD[1], Purnanand V BHALE[1,*]

[1]*Renewable and Sustainable Energy Lab, Department of Mechanical Engineering, Sardar Vallabhbhai National Institute of Technology, Surat, 395 007, India*

ARTICLE INFO

Article history
Received: 07 January 2023
Revised: 28 March 2023
Accepted: 29 March 2023

Keywords:
Electrical Efficiency; PV/T; Solar Cell; Temperature; Water Jacketed Cooling System

ABSTRACT

Renewable energy resources are vital for addressing the universal concerns of air quality, energy security, and sustainable development. Solar energy has several benefits over other popular renewable energy sources, such as its accessibility and increased predictability. The device used for conversion of solar energy to electrical energy is known as photovoltaic panel, which is highly sensitive to the temperature. A significant reduction in efficiency is observed with an increment in temperature hence cooling of photovoltaic panel is highly desirable. Among the different cooling techniques, water cooling is attractive and widely used due to its good thermal properties and availability. Generally, panel cooling through water circulation in tubing is explored in past, however, these tubing structures are having some limitations such as heat transfer barrier, limited surface area, leakage issues, clogging and cost of material. These issues can be partially resolved by using direct contact water jacket cooling system. Therefore, the present study focuses on in enhancing the thermal and electrical characteristics of the solar photovoltaic module through a direct contact water jacketed cooling system.
Initially, a 3D numerical model is developed and the outcome of the numerical model is compared with the experimental work. The results obtained are found in good agreement for solar cell temperature and water outlet temperature. The solar panel performance is investigated with different flow rates such as 0.01, 0.05, 0.1 and 1 cm/s. The direct contact water jacketed cooling system offers simplicity, light weight and cost effectiveness and is found promising over the indirect system. Temperature reduction up to 20 °C is observed over uncooled PV panel whereas enhancement in electrical efficiency up to 9.6 % is observed. The cooled PV solar cell maintain 40.2% low temperature compare to uncooled solar cell temperature.

Cite this article as: Sharma DK, Rathod MK, Bhale PV. Enhancement in thermal and electrical characteristics of solar photovoltaic module through a direct contact water jacketed cooling system. J Ther Eng 2024;10(2):360−374.

***Corresponding author.**
*E-mail address: pvbhale@med.svnit.ac.in

This paper was recommended for publication in revised form by Editor-in-Chief Ahmet Selim Dalkılıç

Published by Yıldız Technical University Press, İstanbul, Turkey

INTRODUCTION

The production of energy from burning of fossil fuels leads to the release of a considerable quantity of greenhouse gases, which contribute to air pollution and global warming of the planet. The need for clean and renewable energy solutions has increased to lessen dependence on fossil-based energy sources. Solar energy is one of the best options for renewable sources because of its availability, cleanliness, and sustainability [1-3]. Firstly, in 1839, the photovoltaic effect was discovered by Edmond Becquerel [4]. The effect of light on a silver-coated platinum electrode immersed in an electrolyte was shown to generate an electric current. A photovoltaic cell converts solar energy (photons) into electricity through a semiconductor band gaps. External and internal variables impact solar panels' performance [5]. Uncontrollable external elements include wind velocity, incoming solar radiation, ambient temperature, and dust deposition on the PV. The internal elements can be regulated, such as the temperature of the PV surface. The decreased output voltage, fill factor, and power output of PV cells are all influenced by increased operational temperature. The band gap of the PV reduces as the temperature of solar cell rises, resulting in an increase in short-circuit current and a drop in open-circuit voltage [6]. Cooling down the temperature of the photovoltaic cell is essential to overcome this problem. Different active and passive cooling techniques are applied to maintain a low operating temperature. It is necessary to remove the heat accumulated on the PV module and use it for other applications to effectively utilize the available solar radiation and increase the PV module efficiency [7-11]. PV/T system utilizes the maximum amount of solar radiation to lower the working temperature and use heat in other applications. Under normal operating cell temperature, a polycrystalline PV panel's electrical efficiency is 13-17% and rest is converted to heat [12-19].

Due to non-uniform temperature distribution, solar cell efficiency decreases and thermal fatigue induced [20]. Generally, it is observed that electrical efficiency decreases by 0.4%– 0.5% for every 1°C increase in solar cell temperature [21]. Pang et al. [22] conducted experiments with a high mass flow rate (0.25 kg/s) to evaluate the PV/T system's thermal and electrical performance. The findings show that the PV/T system's electrical and thermal efficiency increased by 11% and 57%, respectively. The PV/T collector with a sheet-tube construction mounted at a 25° angle showed the best performance at a mass flow rate of 0.15 kg/s. Hachicha et al. [23] performed experimental and numerical study on PV/T system. And found 15% increment in power generation and maintain 16°C lower temperature with respect to uncooled solar panel. Electrical efficiency was increased by 18.3% due to both side cooling.

Vaishak and Bhale [24] investigated the effect of dust accumulation numerically and experimentally on the performance of solar-assisted heat pump (SAHP) system. Around eight-week study in Indian climatic conditions was performed. It was reported that decrease in spectral transmittance from 91% to 46% in the glass, reduced electrical efficiency by 44.14% and the COP of the system by 8.53%. Hachicha et al. [25] based on experimental investigation, highlighted the impact of dust on the energy output of PV panels in the Sharjah climate. The authors found that, based on a 5-month study period when the dust density was 5.44 g/m^2, power reduced by 12.7%.

Solanki et al. [26] performed numerical and experimental study of PV/T solar air heater and observed electrical efficiency of 8.4% and thermal efficiency of 42%. The limited heat conductivity of air contributes to the poor electrical efficiency of air-based PV/T. Sheyda et al. [27] designed and fabricated a laboratory setup to lower PV panel module temperature and enhance output power in Kermanshah, Iran. Wind tunnel ventilation system was used for cooling of the solar panel. Teo et al. [28] carried out an experimental study of PV/T with fins using air blower is used to improve the heat transfer rate. According to the findings, an uncooled panel's temperature reached 68°C, while its electrical efficiency had decreased to 8.6%. By taking advantage of the use of a blower, an operating temperature was obtained around 38°C. Mohammad et al. [29] presented review article which covered almost all recent advancements in efficiency enhancements of photovoltaic panel through single cooling fluid, dual fluid and nanofluids.

Bahaidarah et al. [30] reported that by cooling a photovoltaic panel, temperature of photovoltaic panel dropped about 20% compared to the temperature of convectional PV panel and 9% increment in electrical efficiency was observed. Hussein et al. [31] reported that by active cooling of PV panel, temperature of PV panel dropped from 78°C to 70°C with an increase in electrical efficiency of solar panel to 9.8% at an optimum mass flow rate of 0.2 kg/sec and thermal efficiency to 12.3%. Deng et al. [32] conducted an experimental investigation on the electrical and thermal performance of photovoltaic/thermal system of four different seasons and found 13.76%, 11.92%, 13.71% and 14.65% of electrical efficiency with 31.62%, 33.07%, 24.99% and 17.24% of thermal efficiency. Nizetic et al. [33] conducted an experimental investigation on photovoltaic panels' water spray cooling technique. An increment of 16.3% in the electrical efficiency of photovoltaic panels was observed whereas the temperature of the photovoltaic panel dropped to 24°C compared to 54°C of a similar un-cooled convectional PV panel.

Chow et al. [34] studied water-based PV/T system, and achieved an electrical efficiency of 10.7% and thermal efficiency of 48%. Liquids are more effective in cooling PV panels than air because of their superior thermal characteristics. Yazdanifard et al [35] deployed a computational model of water-based PV/T system to undertake a parametric study on a water-based PV/T system in laminar and turbulent flow conditions. It was observed that the total

energy and exergy efficiency are higher in turbulent flow case. Ahmed et al. [36] investigated on PV/T to measure electrical and thermal output under 500-800 W/m^2 solar radiation with a different mass flow rate of water from 0.011 kg/s to 0.041 kg/s. Highest performance was observed at 800 W/m^2 and 0.041 kg/s mass flow rate. Fakouriyan et al. [37] developed the experimental setup in Tehran, Iran, to observe the effect of water cooling on the efficiency of a PV/T system. According to the findings the water cooling enhanced the system performance resulting improved electrical, thermal and overall efficiency by 12.3%, 49.4% and 61.7%, respectively. The payback period of a PV/T system found 1.7 years and 8.7 years compared to gas and solar water heater. Smith et al. [38] performed experimental investigation in low concentrated PV using top surface cooling to increase the power output. The continuous flow of water over the top considerably reduced the temperature of the PV panel and kept it clean. As a result, the PV panel's optical efficiency improved.

Vaishak and Bhale [39] conducted experimental research on a 100 Wp PV/T panel using cooling fluid as R-134a refrigerant. The electrical efficiency was found as 15.2% and a coefficient of performance (COP) as 2.96. Comparing the PV/T-SAHP (PV/T solar assisted heat pump) system with air and the water-based system demonstrates that the PV/T-SAHP system is a more dependable supply of hot water than the air and water-based system, particularly under low irradiance circumstances. Zhou et al. [40] performed an experimental study on roll bound PVT heat pump system using R-22 refrigerant. The COP was obtained around 6.16 and electrical efficiency of module 11.8%. But the refrigerant-based systems also have disadvantages such as higher operating cost, refrigerant leakage, unequal refrigerant distribution in evaporator tubes, evaporator coil length, etc.

The literature study reveals several passive and active cooling approaches to the solar panel. Active cooling mainly uses air, water and refrigerants and in passive cooling, phase change material and heat pipe. Every cooling technique has their own advantages and limitations. The refrigerant based cooling system has certain drawbacks as cost, complexity and high power consumption in compressor. Water-based cooling technologies are more efficient, effective, and widely used due to their low cost and easy water availability. However, it is found that water circulation over the PV panel is done through small diameter tubes. The water passing through tubes has several limitations, such as low heat transfer area due to line contact, a complex structure of tubes and high cost, high-pressure drop due to bends and requirement of plate to attach the tubes with panel. The limitations such as clogging of tubes and uneven temperature of the module, pumping power can be eliminated using direct contact water jacket heat recovery unit instead of tubes. Therefore, the present study explores the PV panel with water jacket and performs a parametric analysis.

EXPERIMENTAL SETUP

The commercial 100 W_p PV panel of 36 polycrystalline solar cells are used in series. The overall length and width of the module is 1020 mm×650 mm. The area of solar cell is approximately 0.65 m^2. A hybrid collector, brazed with copper plate and copper tube, and held together with a thermally conductive glue with a high bonding strength, comprises the experimental design of a PV/T collector. The performance of the PV panel is tested under different climate conditions towards due south-facing in Surat (21.1702°N, 72.8311°E), India. The experimental setup for sheet-tube PV/T collector is shown in Figure 1.

The tubing with a total length of 25 meters and 8 mm outer diameter was bent in spiral form (shown in Figure 1b) with the adjacent tube. To reduce heat loss to the environment, the entire system was covered in an aluminium casing with a layer of glass wool insulation at the bottom. Table 1 provides the electrical characteristics of the PV module.

Procedure of Experiment

The experiment was performed for 3 hours' time duration from morning 9 A.M. to 12 P.M. and readings were taken after every 30 minutes. Water was taken from overhead tank and collected in 250 litre water tank. A submersible pump was kept in the 250 litre water tank. Water was flowing in the tube through the pump. In these experiments, water was not circulated, it was only once through pass from the panel. In every 30 minutes, glass temperature and outer outlet temperature were measured. Glass temperature and water outlet temperature were measured from thermal imaging camera (Testo 865) and PT-100 thermocouple. For validation of numerical model except replica of setup was modelled. It was observed that Reynolds number (Re) was less than its critical values (2251< 2300) showing that flow was laminar. The specific uncertainties associated with the various instruments used in the experiment is shown in Table 2.

Methodology

In this section, the 3-D PV and PV/T model are developed. The model helps understand each layer's heat dissipation. First, examine the physical model, which includes each layer's material properties and thickness. The reference PV contains five layers: top glass, EVA layer, solar cell, EVA and bottom glass.

Physical model

The physical model is based on the experimental setup developed by Vaishak and Bhale [39]; the isometric and cross-sectional view is shown in Figure 2.

It consists of top and bottom layers made up of glass with a thickness of 3.2 mm, which provides strength to the panel and prevents light from being reflected. Solar cell is covered by an ethylene-vinyl acetate layer having 0.5 mm thickness, which protects the cell from water

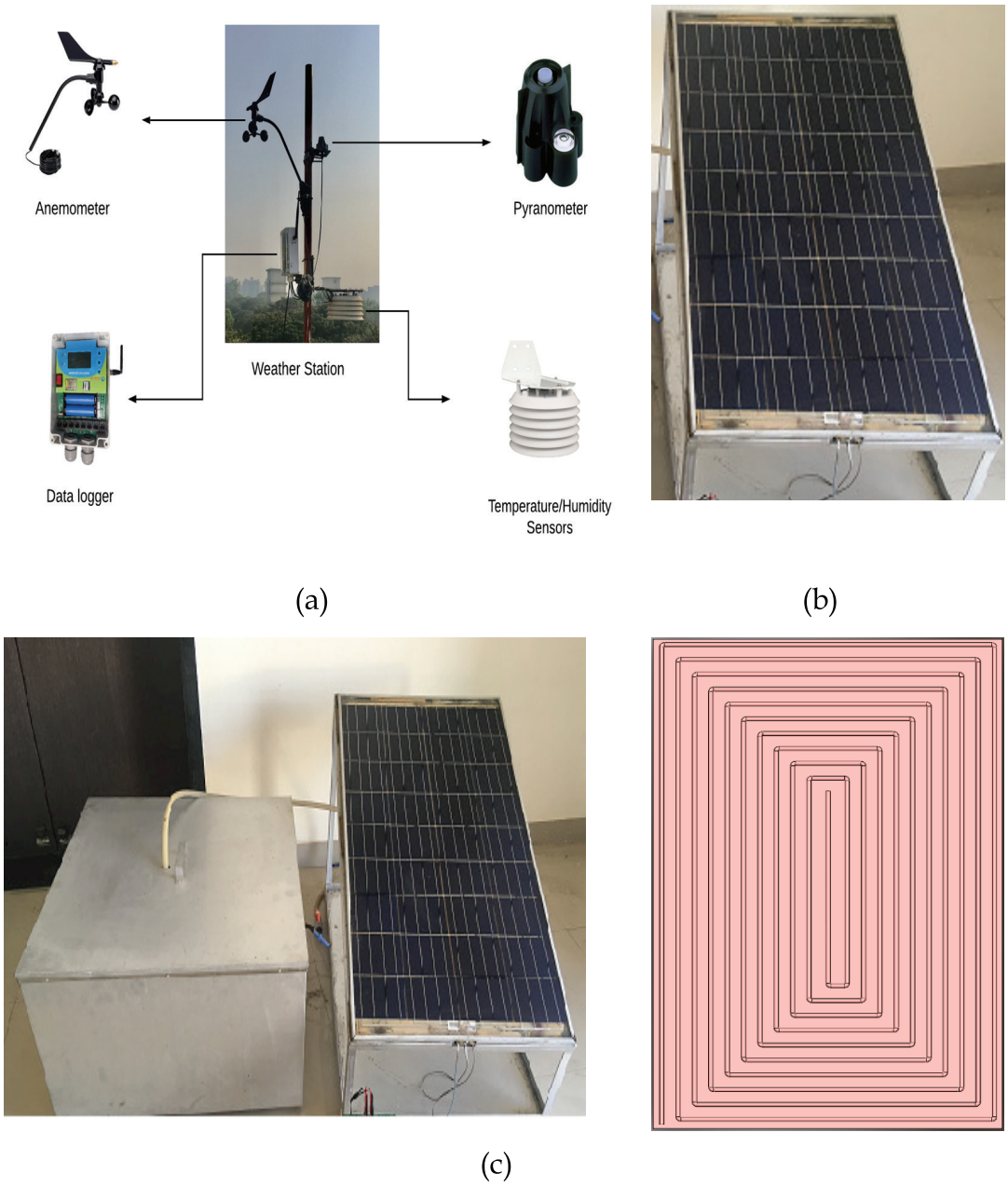

Figure 1. Experimental setup (a) Weather Station (b) Uncooled (refreance) solar panel (c) Water cooled PV with copper tubing on the back side of the module.

Table 1. Electrical characteristics of PV panel

Maximum power	100 W_p
Open circuit voltage	22.2 V
Short circuit current	5.94 A
Current at maximum power	5.40 A
Voltage at maximum power	18.54 V

and from being destroyed. A solar cell has a thickness of 0.3 mm. To establish the performance of solar PV, a mathematical model is developed. Similarly, Figure 3 shows the cross-sectional view and water cooled PV having 10 mm layer thickness.

To avoid the bulkiness of water jacket and leakage issues thickness of 10 mm is considered. Top glass surface may get damaged due to the larger thickness of water jacket. As the temperature of solar cell increases, module efficiency decreases. For maintaining low temperature of the module, fluid at different flow rates and temperatures are used. Water-based cooling technologies are more efficient, work better, and are used more often because of its cost, easy maintenance. Small tubes circulate water over the PV panel.

Table 2. Uncertainty of measuring instruments

Sr.	Instrument	Range	Variable measured	Uncertainty (%)
1	PT-100 type thermocouple	-200˚C to 850˚C	inlet and outlet flow temperature	± 0.15˚C
2	Thermal imager	-20˚C to 280˚C	solar panel temperature	± 2˚C
3	Weather station	Solar irradiance: 0 to 1800 W/m^2	solar radiation, ambient temperature, and wind velocity	± 5% of full spectrum
		Ambient Temperature: -45°C to 60°C		± 0.5 C
		Wind Speed: 0.5 to 89 m/s		± 1 m/s

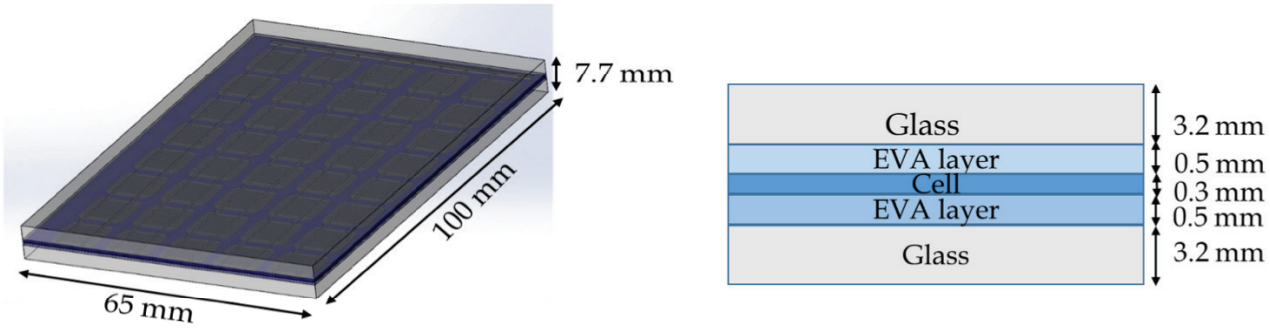

Figure 2. Design of 100 W_p uncooled PV panel and cross-sectional view.

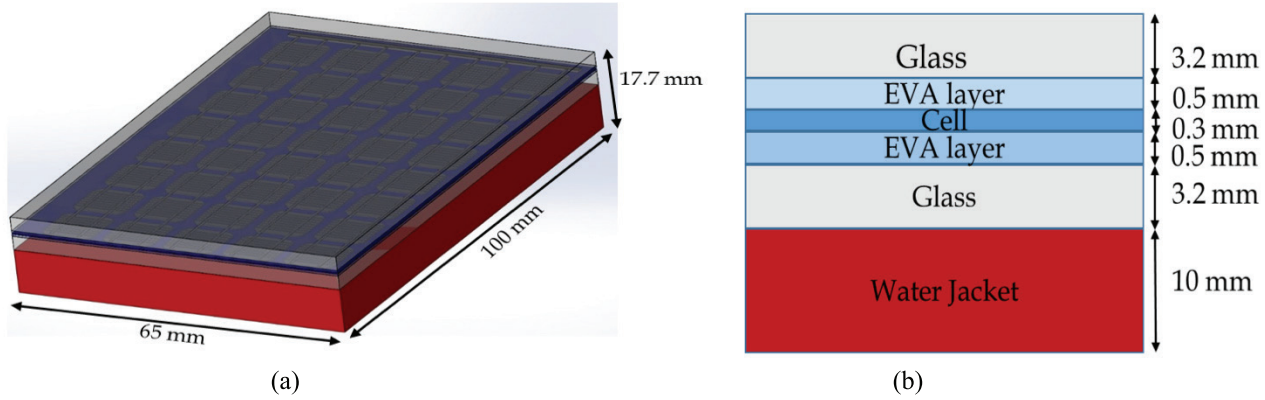

Figure 3. Design of 100 W_p PV with water jacket and a cross-sectional view.

Water running via tubes has various drawbacks, including low heat transfer area due to line contact, complex tube structure, expensive cost, and high-pressure drop due to bends. Water jackets instead of tubes help mitigate these issues.

EVA (ethylene-vinyl acetate) layers at the bottom and top comprise the same material and encapsulate the photovoltaic cells. The uppermost and lowermost layers are composed of glass, and their physical characteristics are identical. Because of this, the model constructed to analyze the thermal behavior of the PV module includes all layers to observe actual behavior. The physical and thermal properties of layers are shown in Table 3.

Table 3. Thermo-physical properties of layers of water-based PV/T [39]

Layer	Thickness (mm)	Absorptivity (α)	Transmissivity (τ)	Thermal conductivity k (W/m-K)	Specific heat C_p (J/kg-K)	Density (Kg/m^3)
Top glass	3.2	0.05	0.91	0.7	500	3000
EVA-1 & 2	0.5	0.08	0.9	0.35	2090	960
Cell	0.3	0.8	0.09	148	677	2330
Bottom glass	3.2	0.05	0.91	0.7	500	3000
Copper plate	0.64			386	381	8978

Mathematical model

A 3D transient mathematical model is developed based on energy balance to analyze the module's functionality and thermal management.

The mathematical model is based on following assumptions,

i) Contact resistance between layers of PV panel is negligible.
ii) No heat generation in the materials of PV layers.
iii) Clear sky radiation is considered in the analysis.
iv) Material properties of glass, EVA, and solar cell remain constant, do not change with temperature.
v) Only top glass surface having heat transfer to the surrounding by convection and radiation. The bottom side of water jacket assume adiabatically.
vi) Hourly average radiation values, ambient temperature and wind velocity are considered input conditions.
vii) Fluid flow is considered as laminar and non-viscous.
viii) Fluid flow velocity is considered as constant with time.

Governing equation

From top glass to bottom glass, the physical heat transfer phenomenon can be described using 3D energy equation [42]

$$\rho_i C_{p_i} \frac{\partial T}{\partial t} = k_i \left(\frac{\partial^2 T}{\partial x^2} + \frac{\partial^2 T}{\partial y^2} + \frac{\partial^2 T}{\partial z^2}\right) \quad (1)$$

Where, T, ρ, C_p, k are temperature, density, specific heat and thermal conductivity respectively. Subscript i represents glass, ethylene-vinyl acetate, or solar cell layer.

Three governing equations for the 3D transient problem, continuity, momentum, and energy, are considered, which can be described below [42].

Continuity equation:

$$\frac{\partial u}{\partial t} + \frac{\partial(\rho u)}{\partial x} + \frac{\partial(\rho v)}{\partial y} + \frac{\partial(\rho w)}{\partial z} = 0 \quad (2)$$

Momentum equation:

$$\frac{\partial(\rho u)}{\partial t} + \frac{\partial(\rho uu)}{\partial x} + \frac{\partial(\rho vu)}{\partial y} + \frac{\partial(\rho wu)}{\partial z} = -\frac{\partial p}{\partial x} + \frac{\partial}{\partial x}\left(\mu \frac{\partial u}{\partial x}\right) + \frac{\partial}{\partial y}\left(\mu \frac{\partial u}{\partial y}\right) + \frac{\partial}{\partial z}\left(\mu \frac{\partial u}{\partial z}\right) \quad (3a)$$

$$\frac{\partial(\rho v)}{\partial t} + \frac{\partial(\rho uv)}{\partial x} + \frac{\partial(\rho vv)}{\partial y} + \frac{\partial(\rho wv)}{\partial z} = -\frac{\partial p}{\partial y} + \frac{\partial}{\partial x}\left(\mu \frac{\partial v}{\partial x}\right) + \frac{\partial}{\partial y}\left(\mu \frac{\partial v}{\partial y}\right) + \frac{\partial}{\partial z}\left(\mu \frac{\partial v}{\partial z}\right) \quad (3b)$$

$$\frac{\partial(\rho w)}{\partial t} + \frac{\partial(\rho uw)}{\partial x} + \frac{\partial(\rho vw)}{\partial y} + \frac{\partial(\rho ww)}{\partial z} = -\frac{\partial p}{\partial z} + \frac{\partial}{\partial x}\left(\mu \frac{\partial w}{\partial x}\right) + \frac{\partial}{\partial y}\left(\mu \frac{\partial w}{\partial y}\right) + \frac{\partial}{\partial z}\left(\mu \frac{\partial w}{\partial z}\right) \quad (3c)$$

Energy equation:

$$\rho C_p \frac{\partial T}{\partial t} = \frac{\partial}{\partial x}\left(k \frac{\partial T}{\partial x}\right) + \frac{\partial}{\partial y}\left(k \frac{\partial T}{\partial y}\right) + \frac{\partial}{\partial z}\left(k \frac{\partial T}{\partial z}\right) + q \quad (4)$$

Where q is the heat flux coming in the solar cell through irradiation. It is incorporated from the UDF in boundary conditions. u, v, and w are velocities in x, y and z direction. ρ, Cp, p and μ are the material›s density, specific heat, pressure and dynamic viscosity.

Boundary conditions

The following provides an explanation of the boundary conditions used in the computation of the domain: Boundary conditions for the calculation of the domain are as follows,

At the exterior surface of solar PV, which is exposed to convective heat transfer

$$\dot{q} = \alpha I_t + \alpha\tau I_t + \in \sigma\left({T_{sky}}^4 - T_g^4\right) + h_0\left(T_\infty - T_g\right) \quad (5)$$

$$-K_i \frac{\partial T}{\partial \eta} = h_o(T_S - To)$$

$$ho_{convective} = 2.8 + 3V_{wind} \text{ for } V_{wind} < 3 \text{ m/s [22]} \quad (6)$$

where V_{wind} = wind velocity in (m/s)

$$T_{sky} = 0.0552{T_o}^{1.5} \text{ for clear sky [23]} \quad (7)$$

$$T_{sky} = T_o \text{ for cloudy sky [23]} \quad (8)$$

Where, T = Temperature of top glass surface at time t
Exterior surface jacket exposed to adiabatic condition

$$\frac{\partial T}{\partial \eta} = 0 \tag{9}$$

$$\eta = \eta_{ref}\left[1 - \beta_{ref}\left(T_{pv} - T_{ref}\right)\right] \tag{10}$$

For reference operating conditions, PV cells use module electrical efficiency (η_{ref}) at the standard test condition, for study taken 13%. The reference temperature condition T_{ref} is 25°C, β_{ref} reference temperature coefficient and its value is taken as 0.00392 /K, respectively [22, 23]. Thus, the total power output is given by:

$$P_{out} = \eta_{ref}\left[1 - \beta_{ref}\left(T_{pv} - T_{ref}\right)\right] \times A \times G_T \tag{11}$$

Computational methodology

A commercial computational software ANSYS is used for the numerical work. The 3-D model is created using a geometrical model Design modeller and simulated using Fluent 18.1. To calculate the velocity and pressure field, Semi-Implicit Pressure-Linked Equation (SIMPLE) algorithm established by Patankar and Spalding [42] is used. For discretization, second-order upwind scheme is used for momentum and energy equation. Similarly, PRESTO (PREssure STaggering Option) scheme is used for pressure discretization. Convergence criteria for continuity, momentum, and energy equation are set to 10^{-6} and 10^{-8}. Figure 4 shows the geometrical model of direct jacketed PV cooling system. It also shows the meshed geometry with hexahedral elements. A User Defined Function (UDF) developed in C++ is used to incorporate both radiative and convective solar panel boundaries. UDF is attached to the solver for adopting combined boundary conditions in the simulations.

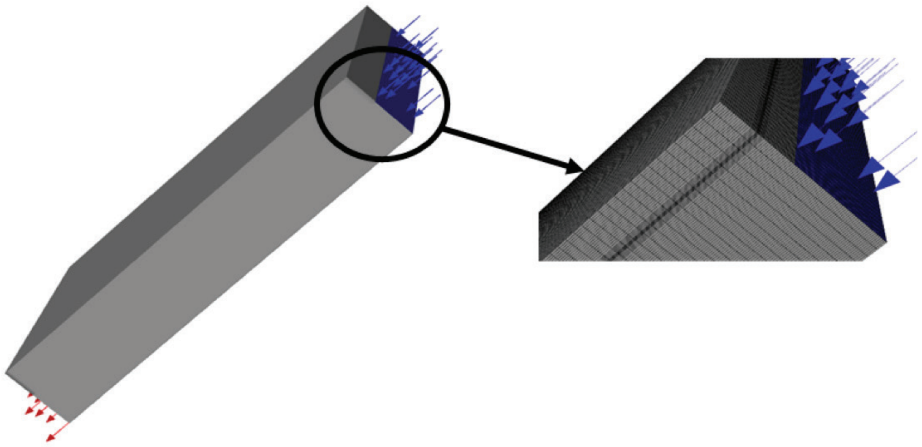

Figure 4. Geometrical model and mesh of direct jacketed PV cooling system.

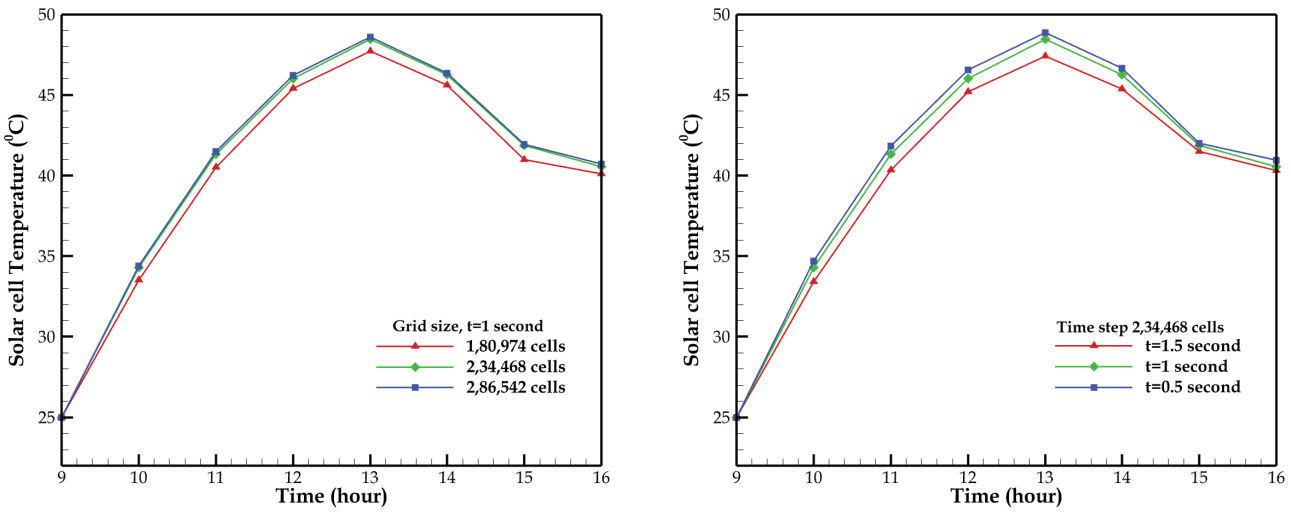

(a) (b)

Figure 5. Transient solar cell temperature with various (a) grid size & (b) time step size.

Grid and time step independence study

The grid size and time step independent study is carried out, so an accurate outcome can be achieved with minimal computational power. Three different grid size with 1,80,974 cells, 2,34,468 cells and 2,86,542 cells are considered for present study. The Figure 5(a) shows the value of transient solar cell temperature with three different considered grid sizes, and it is observed that temperatures with 2,34,468 and 2,86,542 are almost similar. Therefore, a grid size with 2,34,468 number of cells is selected for the further numerical study.

Three different time step size with 0.5 second, 1 second and 1.5 second are also considered for the present work. The figure 5(b) shows the value of transient solar cell temperature with three different time step size, and it is observed that temperatures of 1 second and 0.5 second are almost identical. Therefore, time step 1 second is selected for further numerical work. Overall the combination of 2,34,468 number of cells with 1 second time step is used for the numerical study.

VALIDATION OF NUMERICAL MODEL WITH EXPERIMENTAL STUDY

Experiments were performed at S V National Institute of Technology Surat, India. PV Panel is mounted on a frame whose tilt angle is 22°. The Figure 1(a) shows a photograph of the 100 Watt double glass polycrystalline solar PV panel, which is 0.65 m^2. The performance of the PV

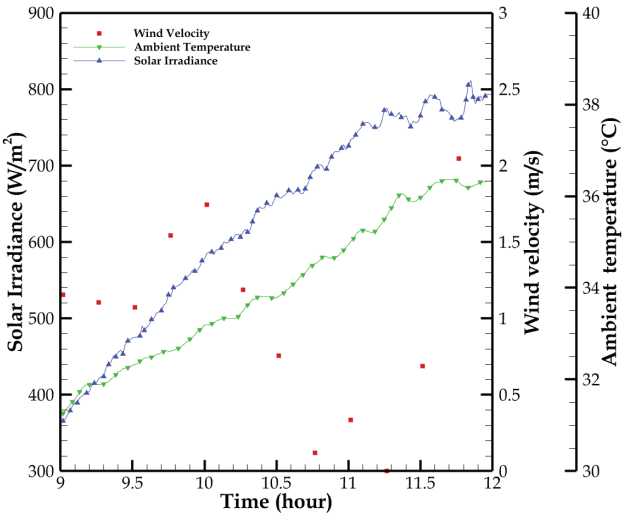

Figure 6. Representation of weather data 15th April 2021 for the city Surat.

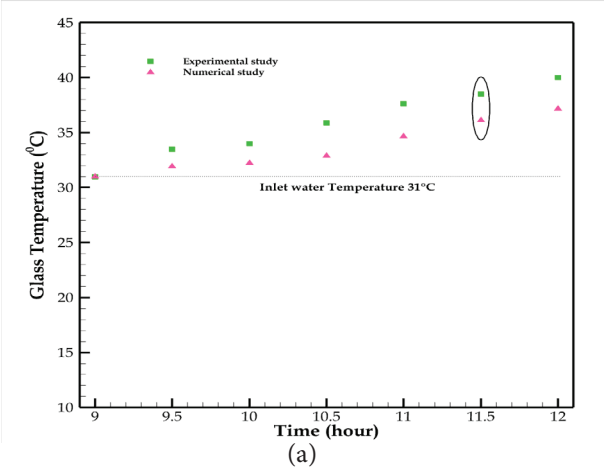

(a)

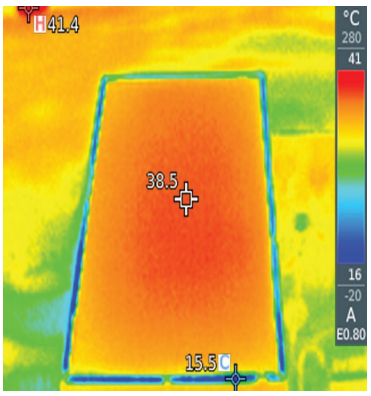

Experimental Study

(b)

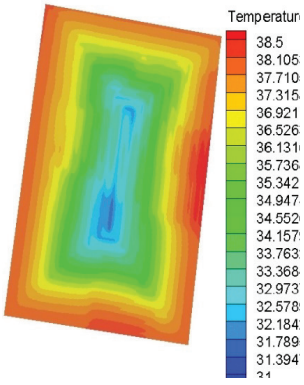

Numerical Study

(c)

Figure 7. Comparison of glass temperature of numerical model with experimental study.

panel was tested on 15th April 2021 under climate conditions due to south-facing in Surat (21.1702°N, 72.8311°E), India. The weather data was taken from the weather station (Davis class B) installed on the terrace of Renewable and Sustainable Energy Lab. The weather data, including insolation, ambient temperature and wind velocity, are represented in Figure 6.

The radiation intensity varies from 365 W/m2 to 811 W/m2 and the maximum radiation was achieved at 11.51 A.M., similarly ambient temperature ranging from 31°C to 36°C, and maximum temperature was reached at 11.42 A.M. The wind velocity varies from 0 to 2 m/s. Maximum velocity observed at 10.50 A.M. Figure 7 represents the transient glass temperature variation of experimental and numerical results. The temperature counters of experimental and numerical study have shown instant at 11.30 A.M.

Actual glass temperature captured by thermal imaging camera which is shown in Figure 7(b). The numerical study counter is shown in Figure 7(c). Experimental reading shows the average temperature is 38.5°C and a numerical study predicted 36.1°C average temperature. The approximate error is 6.22% which represents the simulation results are consistent with the test result.

Figure 8 represents the transient water outlet temperature with the experimental and numerical study. It is assumed that water inlet temperature is constant throughout the study. The maximum water temperature obtained at the 12 P.M. was 40.9°C and the predicted temperature through model was 38.4°C. Comparison of water outlet temperature between experimental result and simulated result to validate the numerical model. The approximate error is 6.11%. It is observed that both glass temperature and water outlet temperature relative error are less the 10%. The analysis reveals that the simulation results are consistent with the test result. Therefore, this model can be regarded as adequate and precise enough to simulate the temperature of the PV.

RESULTS AND DISCUSSION

The purpose of the numerical simulation is to investigate the impact of varying the cooling water temperature on the thermal behavior of the PV/T cooling model.

This complete study is performed based on weather data of 16th February 2022 of Surat city, shown in Figure 9. It shows the day's solar radiation, ambient temperature and wind velocity variation. The weather data was taken from the weather station (Davis class B) installed at Surat (21.17°N, 72.83°E). The solar radiation increased from 100 W/m^2 at 9 hours and reached its peak value of 821 W/m^2 around 2 P.M. It decreased to 638 W/m^2 at 4 P.M. The wind velocity was observed up to 0.2 m/s and maximum temperature was observed 28.8°C. Weather data had taken in clear sky day.

Effect of Still Water Temperature

These studies were performed from morning 9 A.M. to afternoon 4 P.M. The water is filled in an enclosure to the back side of the module and observed the effect on penal temperature.

Figure 10 represents the solar cell temperature variation with different cooling water temperature. In these studies, water temperature varies from 5°C to 25°C with an interval of 5°C. The reference PV obtained maximum temperature 48.5°C, at 1 P.M. And remaining all case obtained maximum temperature of approximate 42°C, at 2 P.M. Firstly the temperature goes down up to 10 A.M. in case of 5°C

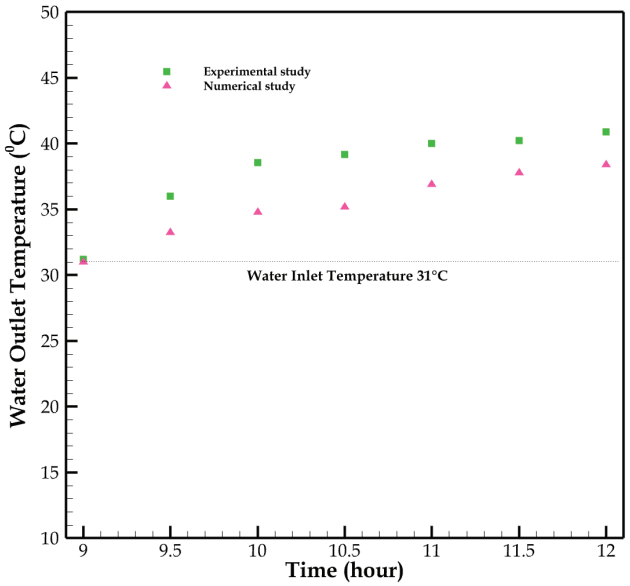

Figure 8. Comparison of water outlet temperature of numerical model with experimental study.

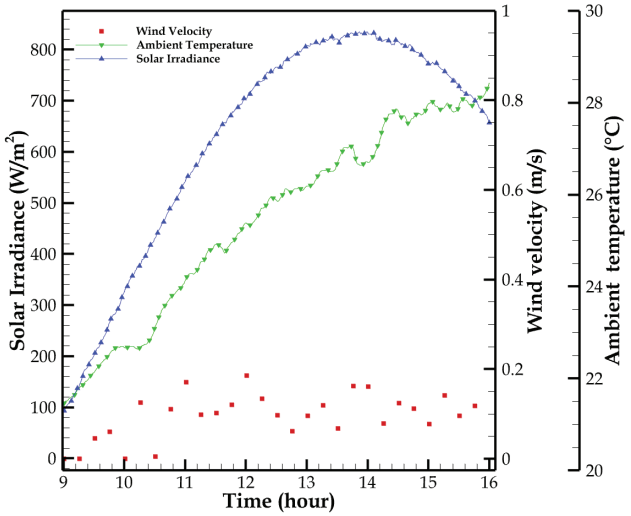

Figure 9. Representation of weather data of 16th Feb 2022 for city Surat.

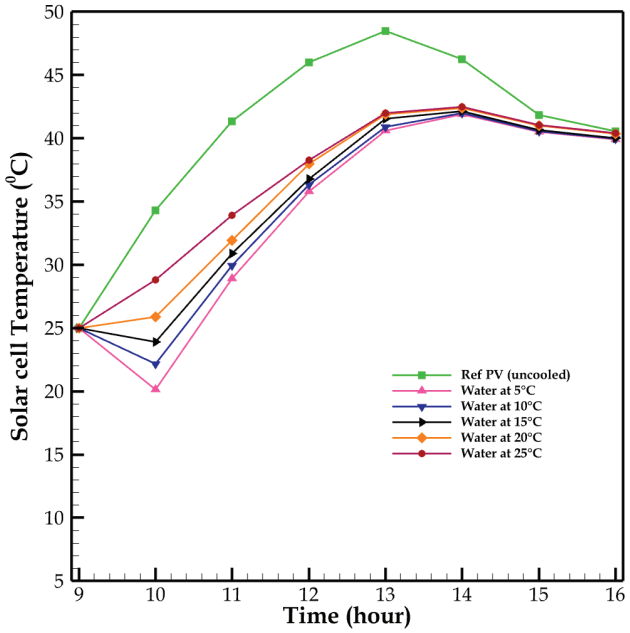

Figure 10. Transient solar cell temperature with different temperatures of still water.

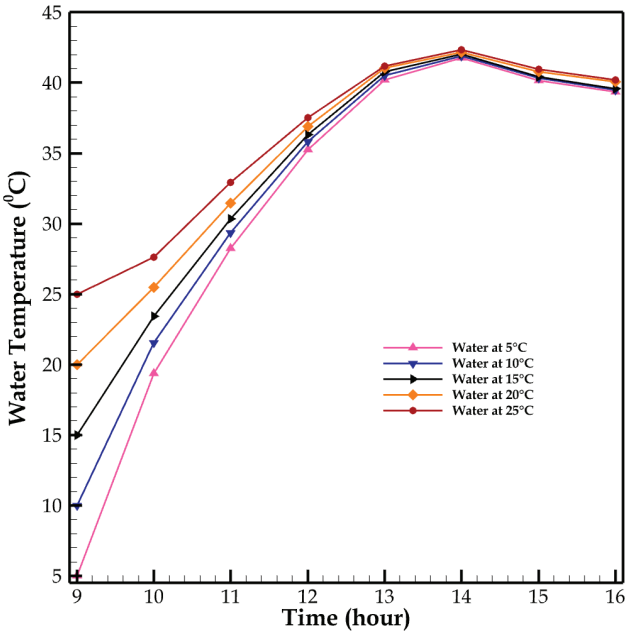

Figure 11. Transient water temperature with different temperature of still water.

to 20°C water temperature because initialization is done at 25°C. So due to cooling fluid temperature solar panel temperature decreases. The maximum deviation observed at 10 A.M. cell temperature was of 20.1°C in case of water at 5°C and 28.8°C in case of water at 25°C. The difference was observed 28.72% more compared in steady water cases at 10 A.M., similarly 5°C of water maintains temperature of 69.15% lower than the reference case. It is observed that difference continually decreases and at 2 P.M. the maximum difference is only 1%. It is observed that all cases, including reference condition temperature almost same at 4 P.M. These is happed because, water is started reverse heating of the module. Because water is reached almost same temperature of the module.

The variation in water temperature with time is illustrated in Figure 11. Five different water temperatures from 5°C to 25°C are investigated. The transient water temperature increases because radiation availability increases. The difference of water temperature continuously decreases; at 2 P.M., it is approximately 0.95% only. So it is observed that these cooling techniques are not very effective because after 2-hour temperature of PV modules are almost the same. Because of these it is not a preferable way of cooling technique. No need to cool down water up to low temperature. It is not good from energy and economical point of view also. According to these study it is observed that 5°C and 25°C stationary water is providing nearly same results.

Effect of Flowing Water on Thermal Performance of PV

In this study, 25°C water temperature is considered and the flow with different velocities is varying from 1 cm/s to

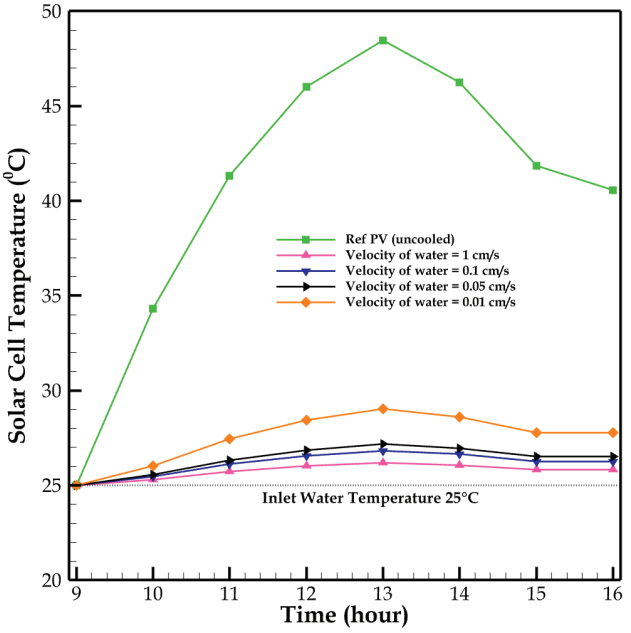

Figure 12. Transient temperature of solar cell once through with different velocity of water in jacket.

0.01 cm/s. These studies observed that as the velocity of water decreased, solar cell temperature increased.

Due to retention time is increased, so carrying capacity is increased. The observation is based on once trough passes the water through the cooling jacket. The transient solar cell temperature with various velocities of flowing

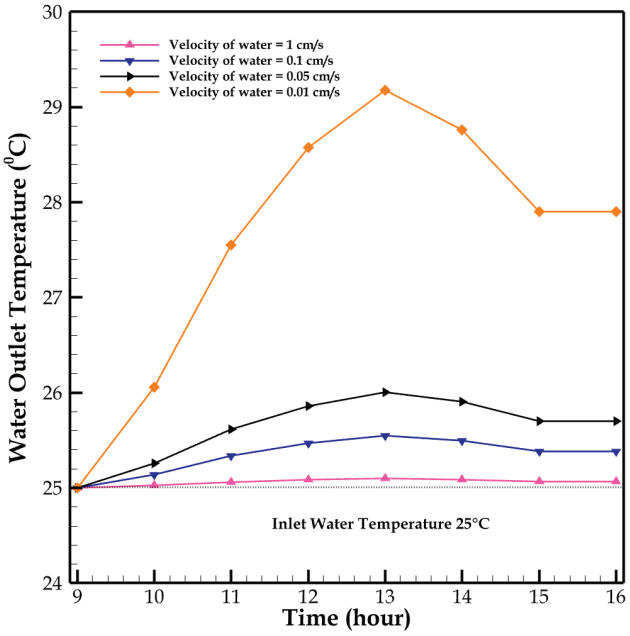

Figure 13. Transient water outlet temperature once through with different velocity of water in jacket.

water is shown in Figure 12. It shows water moving with a velocity 1 cm/s is maintaining almost 25°C throughout the day. It happens because velocity is very high and duct width is only 10 mm. So it will not able to capture the heat because resistance time contact is significantly less. But in the case of velocity 0.01 cm/s, cell temperature varies from 25°C to 29.1°C. The maximum temperature achieved at 1 P.M. It is to be noted that maximum temperature 48.5°C achieved by uncooled PV.

Figure 13 shows the transient water outlet temperature with velocities of water. The complete study is observed during the once-through passing of fluid. Maximum 29.2°C water temperature reached at 1 P.M. with a velocity of 0.01 cm/s. It is observed that 16.2% increment in temperature rise with 0.01 cm/s compare to 1 cm/s at 1 P.M. in single pass. The panel performance is also not affected because the temperature is nearly (standard test condition) STC condition. So negligible thermal stresses are generated compared to an uncooled solar panel.

Figure 14 depicts the counters of average PV cell temperature with time. It represents the temperature of the module varying between 25°C to 29°C between these durations when velocity of water changes from 1 cm/s to 0.01 cm/s. At 9 A.M. all cases at initial temperature is 25°C. It is observed from counter the maximum temperature obtained at 1 P.M. after it is decreases and its maximum temperature is around 29°C. After 1 P.M. radiation decreases so the module's temperature starts decreasing. This study observed that 0.01 cm/s provides the best results and the lowest pumping power among all cases.

It provides more uniform cooling compared to fluid flowing through tube. The findings indicate that the circular pipe's flow is insufficient to cool the panel uniformly. The panel's temperature differential occurs because the working fluid grows warmer as it travels down the pipe and cools the panel, which reduces the heat transfer by decreasing the temperature difference between the solar panel and heated working fluid.

It also depicts that meagre flow resistance is less compared to pipe flow. More heat transfer occurred because cooling fluid is directly in contact with the PV module. Because in pipe flow extra resistance increases, such as tube welded with plate. Because of tube it is line contact with the panel. So uniform cooling is not provided. If high thermal conductive material is selected for better heat transfer such as copper. It is not good from an economical point of view as well as due to adding resistance, the heat transfer rate also decreases. This shows cooling water jacket is superior to the water flow tube condition from a heat transfer point of view as well as pumping power consumption.

Electrical Conversion Efficiency of PV Cell

The electric conversion efficiency of PV panels mainly depends on temperature. Open-circuit voltage decreases and short-circuit current increases but the rate of decrement of open-circuit voltage is very high compared to a rate of increment in short-circuit current. Hence electric conversion efficiency increases with a decrease in the temperature of PV cell. Figure 15 depicts the transient electrical efficiency of all cases.

The study is performed from morning 9 A.M. to afternoon 4 P.M. with the Indian climate condition in the winter season. The solar irradiance was observed 202-822 W/m^2, while the ambient temperature varied between 21.5°C and 28.8°C.

The above result shows that the uncooled PV module has the lowest efficiency because it has the highest temperature in complete duration. And the highest efficiency is achieved in the case of a flowing velocity of 1 cm/s cooling fluid because it has high heat carrying capacity. It depicts the efficiency of solar cells with 1 cm/s velocity at 1 PM 9.6% more efficient compare to uncooled PV.

Electrical Power Output of PV Cell

Figure 16 represents the power output of the solar PV with the time. It shows that as the radiation intensity increases, power generation from the cell also increases. But the solar penal temperature also increases which produce a negative power coefficient. So power output is decreases for improving the power of module cooling is required. Water flowing with 1 cm/s produces maximum power because it has maximum heat carrying capacity compare to other case. It is observed that at 1 P.M. 9.6% more power generation in 1 cm/s flowing water condition. This complete study is under once through the passing of the liquid.

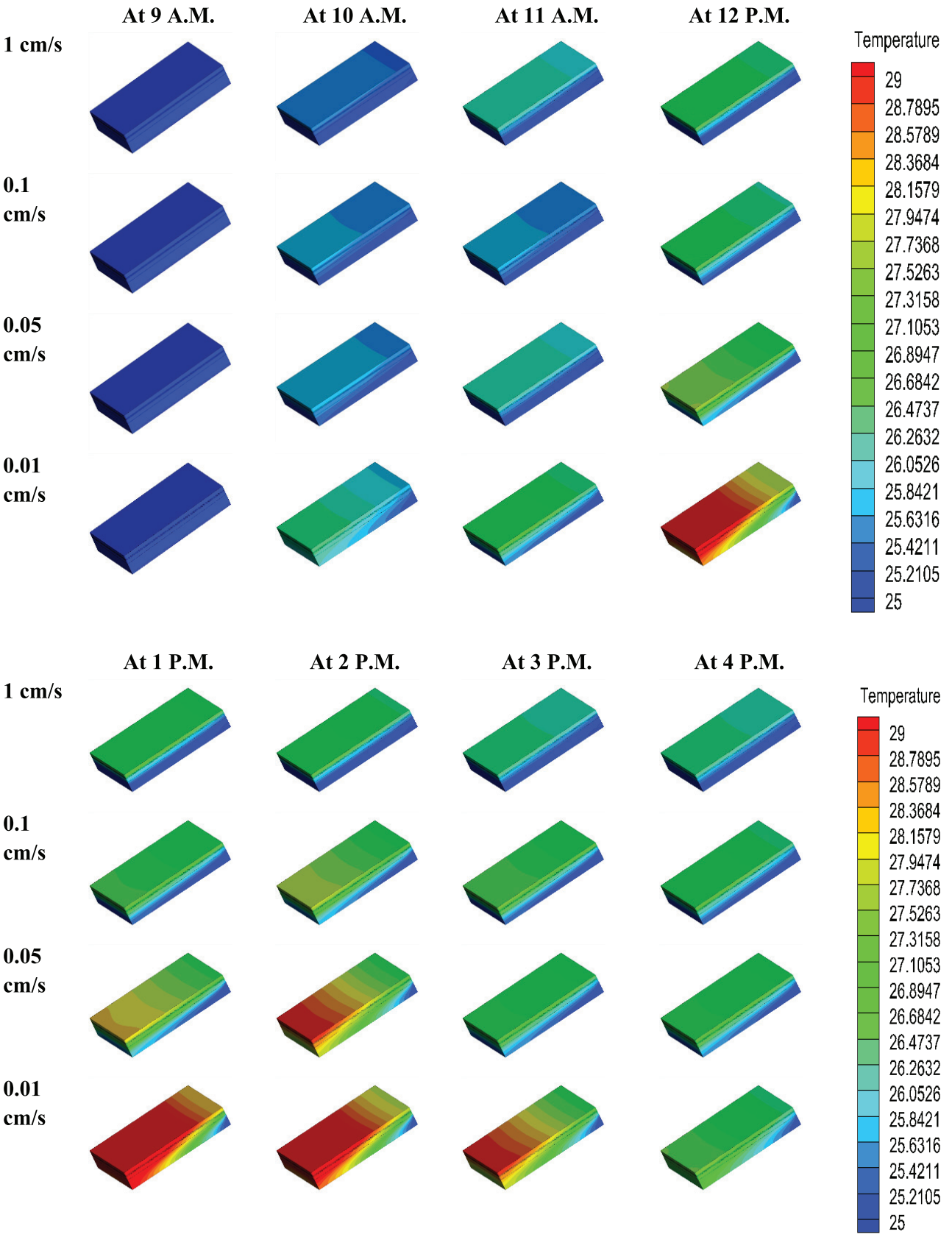

Figure 14. Transient temperature counters of once through different flow rate with time of water in jacket.

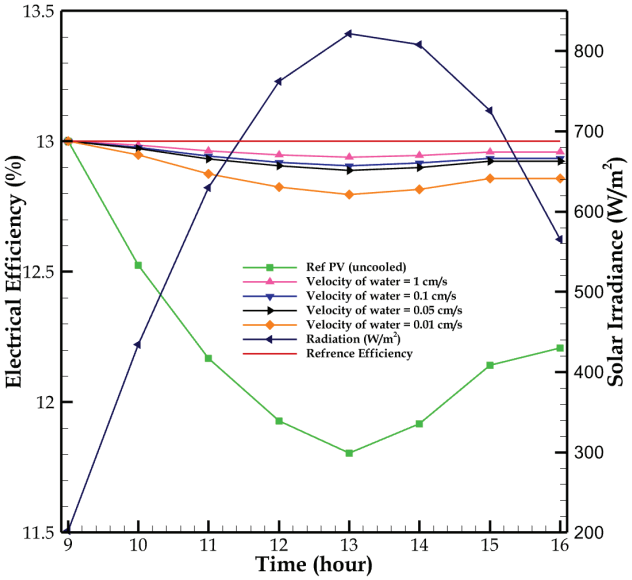

Figure 15. Transient variation of electrical efficiency with once through different velocity of water.

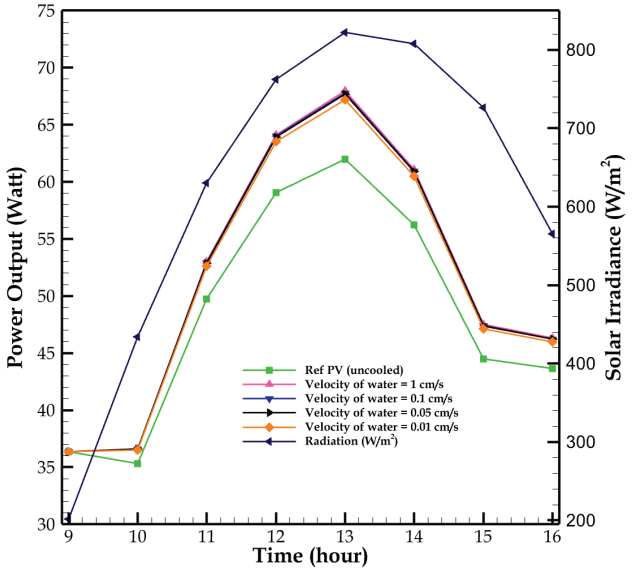

Figure 16. Transient variation of power output with once through different velocity of water.

CONCLUSION

In this study, a three-dimensional numerical model has been developed using ANSYS Fluent and evaluate its results against those obtained from experiment. The performance of solar panels is evaluated with different flow rates, such as 0.01, 0.05, 0.1, and 1 cm/s. Direct contact water jacketed cooling systems are simpler, lighter, and cheaper than indirect systems. The main disadvantages of water-based PV/T using copper plate and tubing are higher cost, non-uniform cooling, lower performance, more bulkiness and higher maintenance. These issues are addressed through a simple, light weight, direct contact jacket type cooling system with improved electrical and thermal characteristics. The specific findings are listed here.

- The cooled PV solar cell maintain 40.2% low temperature compare to uncooled solar cell temperature.
- Almost 20°C temperature difference are maintaining water cooled PV with reference Photovoltaic panel temperature.
- Flowing water in a jacket shows better results than still water. But if the speed is higher, the water will not carry heat as well. Water moving slowly (0.01 cm/s) gives the best results. And in a single pass, the temperature increased by about 4°C.
- The water flow in the direct contact water jacket provides the optimal conditions for heat transfer, as well as economic and constructional perspectives. The reason for this is that the fluid used for cooling is in direct touch with the back sheet of the solar panel, and the amount of electricity required for pumping is correspondingly quite low.
- Highest power production and efficiency of solar cells are measured in the condition of 1 cm/s flowing water. The efficiency at 1 p.m. is 9.6% higher than that of uncooled PV.

NOMENCLATURE

A	Area of PV module (m²)
C_p	Specific heat (J/kg-K)
d	Tube diameter (mm)
h	Convective heat transfer coefficient (W/m²-K)
I_t	Total solar radiation (W/m²)
k_i	Thermal conductivity (W/m-K)
L	Length of the coil (m)
$\dot{m}$	Mass flow rate of water (kg/s)
t	Thickness of water jacket (mm)
T	Temperature (°C)
T_o	Ambient temperature (K)
T_{sky}	Sky temperature
T_w	Water temperature in (°C)

Greek symbols

η	Efficiency
α	Absorptivity of the surface
β_{ref}	Reference temperature coefficient
$\in$	Emissivity of glass
σ	Stefan Boltzmann constant
μ	Viscosity (kg/m-s)
ρ	Density of water (kg/m³)
τ	Transmissivity
ΔT	Change in temperature (°C)

Abbreviations

COP	Coefficient of Performance
EVA	Ethyl Vinyl Acetate

NOCT	Normal Operating Cell Temperature
PV	Photovoltaic
PV/T	Photovoltaic Thermal
PCM	Phase Change Material
STC	Standard Test Condition
UDF	User Defined Function

AUTHORSHIP CONTRIBUTIONS

Authors equally contributed to this work.

DATA AVAILABILITY STATEMENT

The authors confirm that the data that supports the findings of this study are available within the article. Raw data that support the finding of this study are available from the corresponding author, upon reasonable request.

CONFLICT OF INTEREST

The author declared no potential conflicts of interest with respect to the research, authorship, and/or publication of this article.

ETHICS

There are no ethical issues with the publication of this manuscript.

REFERENCES

[1] Bolaji BO, Huan Z. Ozone depletion and global warming: Case for the use of natural refrigerant-a review. Renew Sustain Energy Rev 2013;18:49−54. [CrossRef]

[2] Allouhi A, Rehman S, Buker MS, Said Z. Up-to-date literature review on Solar PV systems: Technology progress, market status and R&D. J Clean Product 2022;362:132339. [CrossRef]

[3] Demirbas A. Hazardous emissions, global climate change and environmental precautions. Energy Sources Part B: Econ Plan Pol 2006;1:75−84. [CrossRef]

[4] Würfel U, Neher D, Spies A, Albrecht S. Impact of charge transport on current-voltage characteristics and power-conversion efficiency of organic solar cells. Nature Comm 2015;6:1−9. [CrossRef]

[5] Fahrenbruch A, Bube R. Fundamentals of solar cells (Photovoltaic solar energy conversion). J Sol Energy Eng 1984;106:497−498. [CrossRef]

[6] Rachid A, Goren A, Becerra V, Radulovic J, Khanna S. Fundamentals of solar energy. In: Rachid A, Goren A, Becerra V, Radulovic J, Khanna S. Solar Energy Engineering and Applications. New York: Springer International Publishing; 2023. pp. 1−15. [CrossRef]

[7] Panwar NL, Kaushik SC, Kothari S. Role of renewable energy sources in environmental protection: A review. Renew Sustain Energy Rev 2011;15:1513−1524. [CrossRef]

[8] Amelia AR, Irwan YM, Leow WZ, Irwanto M, Safwati I, Zhafarina M. Investigation of the effect temperature on photovoltaic (PV) panel output performance. Int J Adv Sci Eng Inf Technol 2016;6:682−688. [CrossRef]

[9] He Z, Zhong C, Huang X, Wong WY, Wu H, Chen L, et al. Simultaneous enhancement of open-circuit voltage, short-circuit current density, and fill factor in polymer solar cells. Adv Mater 2011;23:4636−4643. [CrossRef]

[10] Chander S, Purohit A, Sharma A, Nehra SP, Dhaka MS. A study on photovoltaic parameters of mono-crystalline silicon solar cell with cell temperature. Energy Rep 2015;1:104−109. [CrossRef]

[11] Said SA, Hassan G, Walwil HM, Al-Aqeeli N. The effect of environmental factors and dust accumulation on photovoltaic modules and dust-accumulation mitigation strategies. Renew Sustain Energy Rev 2018;82:743−760. [CrossRef]

[12] Dwivedi P, Sudhakar K, Soni A, Solomin E, Kirpichnikova I. Advanced cooling techniques of PV modules: A state of art. Case Stud Therm Engineer 2020;21:100674. [CrossRef]

[13] Ciulla G, Lo Brano V, Franzitta V, Trapanese M. Assessment of the operating temperature of crystalline PV modules based on real use conditions. Int J Photoenergy 2014:718315. [CrossRef]

[14] Noxpanco MG, Wilkins J, Riffat S. A review of the recent development of photovoltaic/thermal (PV/T) systems and their applications. Future Cities Environ 2020;6:1−16. [CrossRef]

[15] Vaishak S, Bhale PV. Investigation on the effect of different backsheet materials on performance characteristics of a photovoltaic/thermal (PV/T) system. Renew Energy 2021;168:160−169. [CrossRef]

[16] Yuan Y, Hassan A, Zhou J, Zeng C, Yu M, Emmanuel B. Experimental and numerical investigation on a solar direct-expansion heat pump system employing PV/T & solar thermal collector as evaporator. Energy 2022;254:124312. [CrossRef]

[17] Rajvikram M, Leoponraj S, Ramkumar S, Akshaya H, Dheeraj A. Experimental investigation on the abasement of operating temperature in solar photovoltaic panel using PCM and aluminium. Solar Energy 2020;188:327−338. [CrossRef]

[18] Preet S, Bhushan B, Mahajan T. Experimental investigation of water based photovoltaic/thermal (PV/T) system with and without phase change material (PCM). Solar Energy 2017;155:1104−1112. [CrossRef]

[19] Vaishak S, Bhale PV. Photovoltaic/thermal-solar assisted heat pump system: Current status and future prospects. Solar Energy 2019;189:268−284. [CrossRef]

[20] Zhou J, Ke H, Deng X. Experimental and CFD investigation on temperature distribution of a serpentine tube type photovoltaic/thermal collector. Solar Energy 2018;174:735−742. [CrossRef]

[21] Karthikeyan V, Sirisamphanwong C, Sukchai S, Sahoo SK, Wongwuttanasatian T. Reducing PV module temperature with radiation based PV module incorporating composite phase change material. J Energy Storage 2020;29:101346. [CrossRef]
[22] Pang W, Cui Y, Zhang Q, Yu H, Zhang L, Yan H. Experimental effect of high mass flow rate and volume cooling on performance of a water-type PV/T collector. Solar Energy 2019;188:1360−1368. [CrossRef]
[23] Hachicha AA, Abo-Zahhad EM, Said Z, Rahman SMA. Numerical and experimental investigations of the electrical and thermal performances of a novel PV thermal system. Renewable Energy 2022;195:990−1000. [CrossRef]
[24] Vaishak S, Bhale PV. Effect of dust deposition on performance characteristics of a refrigerant based photovoltaic/thermal system. Sustain Energy Technol Assess 2019;36:100548. [CrossRef]
[25] Hachicha AA, Al-Sawafta I, Said Z. Impact of dust on the performance of solar photovoltaic (PV) systems under United Arab Emirates weather conditions. Renewable Energ 2019;141:287−297. [CrossRef]
[26] Solanki SC, Dubey S, Tiwari A. Indoor simulation and testing of photovoltaic thermal (PV/T) air collectors. Appl Energy 2009;86:24212428. [CrossRef]
[27] Valeh-e-Sheyda P, Rahimi M, Parsamoghadam A, Masahi MM. Using a wind-driven ventilator to enhance a photovoltaic cell power generation. Energy Buildings 2014;73:115−119. [CrossRef]
[28] Teo HG, Lee PS, Hawlader MNA. An active cooling system for photovoltaic modules. Appl Energy 2012;90:309−315. [CrossRef]
[29] Esfe MH, Kamyab MH, Valadkhani M. Application of nanofluids and fluids in photovoltaic thermal system: An updated review. Solar Energy 2020;199:796−818. [CrossRef]
[30] Bahaidarah H, Subhan A, Gandhidasan P, Rehman S. Performance evaluation of a PV (photovoltaic) module by back surface water cooling for hot climatic conditions. Energy 2013;59:445−453. [CrossRef]
[31] Hussein HA, Numan AH, Abdulmunem AR. Improving of the photovoltaic/thermal system performance using water cooling technique. Mater Sci Eng 2015;78:1−9. [CrossRef]
[32] Deng Y, Quan Z, Zhao Y, Wang L, Liu Z. Experimental research on the performance of household-type photovoltaic-thermal system based on microheat pipe array in Beijing. Energy Convers Manage 2015;106:1039−1047. [CrossRef]
[33] Nizetic S, Coko D, Yadav A, Cabo FG. Water spray cooling technique applied on a photovoltaic panel: The performance response. Energy Convers Manage 2016;108:287−296. [CrossRef]
[34] Chow TT, He W, Ji J. Hybrid photovoltaic-thermosyphon water heating system for residential application. Solar Energy 2016;80:298−306. [CrossRef]
[35] Yazdanifard F, Bajestan EE, Ameri M. Investigating the performance of a water-based photovoltaic/thermal (PV/T) collector in laminar and turbulent flow regime Renew Energy 2016;99:295−306. [CrossRef]
[36] Fudholi A, Sopian K, Yazdi MH, Ruslan MH, Ibrahim A, Kazem HA. Performance analysis of photovoltaic thermal (PVT) water collectors. Energy Conver Manage 2014;78:641−651. [CrossRef]
[37] Fakouriyan S, Saboohi Y, Fathi A. Experimental analysis of a cooling system effect on photovoltaic panels' efficiency and its preheating water production. Renewable Energy 2019;134:1362−1368. [CrossRef]
[38] Smith MK, Selbak H, Wamser CC, Day NU, Krieske M, Sailor DJ, et al. Water cooling method to improve the performance of field-mounted, insulated, and concentrating photovoltaic modules. J Sol Energy Engineer 2014;136:034503. [CrossRef]
[39] Vaishak S, Bhale PV. Performance analysis of a heat pump-based photovoltaic/thermal (PV/T) system. Clean Technol Environ Pol 2021;23:1121−1133. [CrossRef]
[40] Zhou C, Liang R, Zhang J, Riaz A. Experimental study on the cogeneration performance of roll-bond-PVT heat pump system with single stage compression during summer. Appl Therm Engineer 2019;149:249261. [CrossRef]
[41] Tiwari A, Sodha MS, Chandra A, Joshi JC. Performance evaluation of photovoltaic thermal solar air collector for composite climate of India. Sol Energy Mater Sol Cells 2006;90:175−189. [CrossRef]
[42] Patankar SV, Spalding DB. A calculation procedure for heat, mass and momentum transfer in three-dimensional parabolic flows. Numer Pred Flow Heat Transf Turb Combust 1983:54−73. [CrossRef]
[43] Tiwari GN, Tiwari A. Handbook of Solar Energy: Theory, Analysis and Applications. New York: Springer; 2016. [CrossRef]